PHYSICAL REVIEW D **89,** 094009 (2014)

CP violation in $B \to D\tau\nu_\tau$ using multipion tau decays

Kaoru Hagiwara,[1,*] Mihoko M. Nojiri,[1,2,†] and Yasuhito Sakaki[1,‡]
[1]*KEK Theory Center and Sokendai, Tsukuba, Ibaraki 305-0801, Japan*
[2]*Kavli IPMU (WPI), The University of Tokyo, Kashiwa, Chiba 277-8583, Japan*
(Received 26 March 2014; published 8 May 2014)

Present experimental data shows a 3.8σ-level discrepancy with the standard model in $\bar{B} \to D^{(*)}\tau\bar{\nu}_\tau$. Some new physics models have been considered to explain this discrepancy that propose a possible new source of *CP* violation. In this paper, we construct *CP*-violating observables by using multipion decays in $B \to D\tau\nu_\tau$, and estimate the sensitivity of these observables to generic *CP*-violating operators. We also discuss the possibilities of *CP* violation in leptoquark models and in the type-III two-Higgs-doublet model.

DOI: 10.1103/PhysRevD.89.094009 PACS numbers: 13.20.He, 13.35.Dx, 14.80.Fd

I. INTRODUCTION

The standard model (SM) gives an accurate description of elementary particle phenomena; however, experimental uncertainties about the flavor structure of the third generation are still larger than that for the first and second generations. In the standard model, the charged currents are described by the $\mathrm{SU}(2)_L$ gauge coupling of the left-handed doublets of quarks and leptons, and the Cabibbo-Kobayashi-Maskawa flavor-mixing matrix. Some models beyond the standard model predict different structures. A typical example are two-Higgs-doublet models (2HDMs), which predict charged Higgs contributions, and their couplings are proportional to the fermion masses.

For testing the universality of charged currents among the lepton generations, ratios of the branching fractions are introduced as observables,

$$R(D^{(*)}) = \frac{\mathrm{Br}(\bar{B} \to D^{(*)}\tau\bar{\nu})}{\mathrm{Br}(\bar{B} \to D^{(*)}\ell\bar{\nu})}, \tag{1}$$

where ℓ denotes e or μ. The standard model predictions are given in Refs. [1–7]. The values in Refs. [8,9] are

$$R(D)_{\mathrm{SM}} = 0.305 \pm 0.012, \quad R(D^*)_{\mathrm{SM}} = 0.252 \pm 0.004. \tag{2}$$

Predictions of the minimal supersymmetric standard model are found in Refs. [1–3,10,11], which can significantly affect the semitauonic B decays through the Higgs sector of the type-II 2HDM.

The current experimental data are given by the *BABAR* Collaboration [12,13],

$$\begin{aligned} R(D)_{BABAR} &= 0.440 \pm 0.072, \\ R(D^*)_{BABAR} &= 0.332 \pm 0.030, \end{aligned} \tag{3}$$

with an error correlation of $\rho = -0.27$. These results are inconsistent with the SM of Eq. (2) at 3.4σ, or 99.93% C.L., for the two data points. The type-II 2HDM does not improve the fit, as it is inconsistent with the data at 99.8% C.L. for the optimal value of $m_{H^\pm}/\tan\beta$. The Belle Collaboration also reported measurements [14–16], and the newest results (which are estimated in Ref. [13]) are

$$R(D)_{\mathrm{Belle}} = 0.34 \pm 0.12, \quad R(D^*)_{\mathrm{Belle}} = 0.43 \pm 0.08, \tag{4}$$

where the error correlation value is not given. If we assume the same negative correlation of $\rho = -0.27$, the *BABAR* [Eq. (3)] and Belle [Eq. (4)] data can be combined to give

$$R(D)_{\mathrm{exp}} = 0.42 \pm 0.06, \quad R(D^*)_{\mathrm{exp}} = 0.34 \pm 0.03, \tag{5}$$

with an error correlation of $\rho = -0.26$.[1] The combined data is now inconsistent with the SM prediction (2) at 3.8σ (99.985% C.L.).

Some new physics scenarios that are consistent with the data have been considered in Refs. [4–8,17–22]. All leptoquark models compatible with the SM gauge group were studied in Refs. [9,23]. These models were found to be able to explain the experimental results. The type-III 2HDM can also account for the discrepancy [24]. In Ref. [8], a model-independent analysis was performed and the Wilson coefficients of generic dimension-6 operators—which are favored by the experimental data—were identified. The allowed regions of the coefficients reside on the complex plane, and the imaginary parts induce *CP* violation. In Ref. [25], some observables which are sensitive to *CP* violation were constructed by using the D^* polarization. The fully differential decay rate described by the helicity amplitudes for $\bar{B} \to D^*\ell\bar{\nu}$ are measured in $\bar{B} \to D^*\ell\bar{\nu}$ [26–28].

*kaoru.hagiwara@kek.jp
†nojiri@post.kek.jp
‡sakakiy@post.kek.jp

[1]If the error correlation is set to zero in the Belle data [Eq. (4)], the combined results give $R(D)_{\mathrm{exp}} = 0.41 \pm 0.06$ and $R(D^*)_{\mathrm{exp}} = 0.34 \pm 0.03$ with the correlation $\rho = -0.22$, which is inconsistent with the SM at 3.7σ (99.976% C.L.).

In this paper, we discuss CP-violating observables involving the polarization of vector resonances (ρ, a_1, etc.) produced in the decay of the tau lepton in $B \to D^{(*)}\tau\nu$. In Sec. II, we construct observables which have a sensitivity to CP violation in a general situation, and only consider $B \to D\tau\nu$ for simplicity. In Sec. III, we examine the sensitivities of these observables to two independent imaginary parts of new-physics Wilson coefficients. Furthermore, we examine the CP violation term in three leptoquark models, and the type-III 2HDM. Finaly, we summarize our findings in Sec. IV.

II. FORMALISM

A. Effective Hamiltonian and amplitudes

Assuming that the tau neutrinos are left-handed, we introduce a general effective Hamiltonian that contains all possible four-fermion operators of the lowest dimension for the $b \to c\tau^-\bar{\nu}_\tau(\bar{b} \to \bar{c}\tau^+\nu_\tau)$ transition [8],

$$\mathcal{H}_{\rm eff} = \frac{4G_F}{\sqrt{2}} V_{cb}[(1+C_{V_1})\mathcal{O}_{V_1} + C_{V_2}\mathcal{O}_{V_2} + C_{S_1}\mathcal{O}_{S_1} + C_{S_2}\mathcal{O}_{S_2} + C_T\mathcal{O}_T] + \text{H.c.}, \tag{6}$$

where the four-Fermi operators are defined as

$$\mathcal{O}_{V_1} = (\bar{c}_L\gamma^\mu b_L)(\bar{\tau}_L\gamma_\mu\nu_{\tau L}), \tag{7}$$

$$\mathcal{O}_{V_2} = (\bar{c}_R\gamma^\mu b_R)(\bar{\tau}_L\gamma_\mu\nu_{\tau L}), \tag{8}$$

$$\mathcal{O}_{S_1} = (\bar{c}_L b_R)(\bar{\tau}_R\nu_{\tau L}), \tag{9}$$

$$\mathcal{O}_{S_2} = (\bar{c}_R b_L)(\bar{\tau}_R\nu_{\tau L}), \tag{10}$$

$$\mathcal{O}_T = (\bar{c}_R\sigma^{\mu\nu} b_L)(\bar{\tau}_R\sigma_{\mu\nu}\nu_{\tau L}). \tag{11}$$

We consider the decay process $\bar{B} \to D\tau\bar{\nu}_\tau$ followed by the tau lepton decay into two or three pions via a vector resonance,

$$\bar{B}(p_B) \longrightarrow D(p_D)\tau^-(p_\tau)\bar{\nu}_\tau(p_{\nu_1}) \tag{12a}$$

$$\hookrightarrow V^-(Q_{2,3})\nu_\tau(p_{\nu_2}) \tag{12b}$$

$$\hookrightarrow \pi^-(p_1)\pi^0(p_2) \tag{12c}$$

$$\pi^+(p_1)\pi^-(p_2)\pi^-(p_3) \tag{12d}$$

$$\pi^-(p_1)\pi^0(p_2)\pi^0(p_3), \tag{12e}$$

where V denotes vector resonances. The vector resonances are the ρ and ρ' mesons for the 2π decay (12c) and the a_1 meson for the 3π decay (12d),(12e), whose decay branching fractions are about 26% and 18%, respectively. In the case of the 3π decay, we assign the momentum p_1 to a pion which has a different electric charge from the other two pions. In this paper, $\bar{B} \to D$ denotes $\bar{B}^0 \to D^+$ or $B^- \to D^0$ transitions.

The differential decay rate for the processes $\bar{B} \to D\tau^-\bar{\nu}_\tau \to D\nu_\tau\bar{\nu}_\tau + n\pi$ [Eq. 12] are written as

$$d\Gamma_n = \sum_{\lambda\lambda'} d\Gamma_V^{\lambda\lambda'} |F_n(Q_n^2)|^2 \frac{dQ_n^2}{2\pi} d\Gamma_n^{\lambda\lambda'}, \tag{13}$$

where n is a pion number in the process and Q_n denotes the four-momentum of the vector resonance, $Q_n = \sum_{i=1}^n p_i$. The density-matrix distribution of the vector resonance production can be expressed as[2]

$$d\Gamma_V^{\lambda\lambda'} = \frac{1}{2m_B} d\Phi_4(\bar{B} \to DV\nu\bar{\nu}) \mathcal{M}_V^\lambda \mathcal{M}_V^{\lambda'*}, \tag{14}$$

where $d\Phi_4(\bar{B} \to DV\nu\bar{\nu})$ denotes the invariant four-body phase space for the vector boson of the momentum squared $\sqrt{Q_n^2}$, and the decay matrix elements

$$\mathcal{M}_V^\lambda = (\sqrt{2}G_F)^2 V_{cb}\cos\theta_C \bar{u}(p_{\nu_2})P_+\gamma^\alpha \times \frac{\not{p}_\tau + m_\tau}{p_\tau^2 - m_\tau^2 + im_\tau\Gamma_\tau}\Gamma_{\rm NP}P_- v(p_{\nu_1})\epsilon_\alpha^*(Q_n,\lambda) \tag{15}$$

are given for the vector boson of helicity λ in the rest frame of the $\tau\bar{\nu}$ system, where

$$\Gamma_{\rm NP} = C_V H_V^\mu\gamma_\mu + C_S H_S + C_T H_T^{\mu\nu}\sigma_{\mu\nu} \tag{16}$$

$$= e^{i\arg(C_V)}(|C_V| H_V^\mu\gamma_\mu + \tilde{C}_S H_S + \tilde{C}_T H_T^{\mu\nu}\sigma_{\mu\nu}) \tag{17}$$

gives the $\bar{B} \to D\tau\bar{\nu}_\tau$ matrix elements of the general $b \to c\tau\bar{\nu}_\tau$ contact interactions with new physics contributions.[3] We parametrize the three Wilson coefficients as

$$C_V = 1 + C_{V_1} + C_{V_2}, \qquad C_S = C_{S_1} + C_{S_2}, \qquad \tilde{C}_{S,T} = e^{-i\arg(C_V)} C_{S,T}, \tag{18}$$

where $C_V = 1$ stands for the SM, and we factor out the overall phase of the generalized coefficients C_V. In Eq. (18), $P_\pm = (1 \pm \gamma_5)/2$, θ_C denotes the Cabbibo angle, and $\epsilon^\alpha(Q,\lambda)$ is the polarization vector of vector resonances. The hadronic amplitudes $H_{V,S,T}$ are defined as

[2]As explained in the following section, we perform the numerical analysis by using amplitudes in TAUOLA [29,30], which takes account of the scalar (π') contribution to the 3π mode. Although the scalar contributions can be included in our formalism by introducing the scalar polarization ($\lambda = 4$) of the "vector" resonance, we keep the 3×3 form of the density matrix (with $\lambda, \lambda' = \pm 1, 0$) for the sake of brevity. None of our final results are sensitive to the π' contribution to the 3π channel.

[3]We neglect the new physics effect in the multipion tau decays. No evidences of new physics in the hadronic tau decays exists at the moment [31–33]. Searches for CP violation in the hadronic tau decays have been reported recently [34,35], and future precision measurements for the decay might further constrain the new physics effect.

$$H_V^\mu = \langle D(p_D)|\bar{c}\gamma^\mu b|\bar{B}(p_B)\rangle, \tag{19}$$

$$H_S = \langle D(p_D)|\bar{c}b|\bar{B}(p_B)\rangle, \tag{20}$$

$$H_T^{\mu\nu} = \langle D(p_D)|\bar{c}\sigma^{\mu\nu}(1-\gamma_5)b|\bar{B}(p_B)\rangle. \tag{21}$$

The pseudovector and the pseudoscalar hadronic amplitudes are zero,

$$\langle D|\bar{c}\gamma^\mu\gamma_5 b|\bar{B}\rangle = \langle D|\bar{c}\gamma_5 b|\bar{B}\rangle = 0, \tag{22}$$

due to the parity conservation in the strong interactions. Three hadronic amplitudes in Eqs. (19)–(21) have been parametrized by using the heavy-quark effective theory [36] and have been measured by the *BABAR* and Belle experiments [26–28,37]. We adopt the parametrization given in the Ref. [9] in our numerical analysis.

In Eq. (13), the density matrix of the $V \to n\pi$ decay distribution is defined as

$$d\Gamma_n^{\lambda\lambda'} = d\Phi_n \mathcal{M}_n^\lambda \mathcal{M}_n^{\lambda'*}, \tag{23}$$

where the $V \to n\pi$ decay amplitudes $\mathcal{M}_n^\lambda$ are given in Refs. [29,30,38]. For the 2π decay $V^- \to \pi^-(p_1)\pi^0(p_2)$,

$$\mathcal{M}_2^\lambda = \sqrt{2}\epsilon^\alpha(Q_2,\lambda)(p_1-p_2)_\alpha, \tag{24}$$

and for the 3π decay $V^- \to \pi^+(p_1)\pi^-(p_2)\pi^-(p_3)$ or $\pi^-(p_1)\pi^0(p_2)\pi^0(p_3)$,

$$\mathcal{M}_3^\lambda = \frac{4}{3f_\pi}\epsilon^\alpha(Q_3,\lambda)[F_2(P_{12}^2)(p_1-p_2)_\alpha + F_2(P_{13}^2)(p_1-p_3)_\alpha], \tag{25}$$

with

$$P_{ij} = p_i + p_j. \tag{26}$$

The form factors $F_n(Q_n^2)$ are parametrized in Refs. [29,30] as

$$F_2(Q^2) = [B_\rho(Q^2) + \alpha B_{\rho'}(Q^2)]/(1+\alpha), \tag{27}$$

$$F_3(Q^2) = B_{a_1}(Q^2) \tag{28}$$

by using a modified Breit-Wigner propagator $B_V(Q^2)$,

$$B_V(Q^2) = \frac{m_V^2}{m_V^2 - Q^2 - i\sqrt{Q^2}\Gamma_V(Q^2)}. \tag{29}$$

We consider ρ and ρ' resonances in the case of $V \to 2\pi$ decay, with $\alpha = -0.145$ [29,30] in Eq. (27). The running width is defined as

$$\sqrt{Q^2}\Gamma_V(Q^2) = m_V\Gamma_V\frac{Q^2 g_V(Q^2)}{m_V^2 g_V(m_V^2)}, \tag{30}$$

where the line-shape factors are

$$g_{\rho,\rho'}(Q^2) = \bar{\beta}\left(\frac{m_{\pi^-}^2}{Q^2}, \frac{m_{\pi^0}^2}{Q^2}\right), \tag{31}$$

$$g_{a_1}(Q^2) = \begin{cases} \frac{4.1}{Q^2}(Q^2-9m_\pi^2)^3[1-3.3(Q^2-9m_\pi^2)+5.8(Q^2-9m_\pi^2)^2], & \text{if } Q^2 < (m_\rho+m_\pi)^2 \\ 1.623 + \frac{10.38}{Q^2} - \frac{9.32}{Q^4} + \frac{0.65}{Q^6}, & \text{if } Q^2 > (m_\rho+m_\pi)^2 \end{cases} \tag{32}$$

with

$$\bar{\beta}(a,b) = (1+a^2+b^2-2a-2b-2ab)^{1/2}. \tag{33}$$

B. *CP* asymmetries

We compare $B \to \bar{D}$ processes with $\bar{B} \to D$ processes in Eq. (12),

$$B(p_B) \longrightarrow \bar{D}(p_D)\tau^+(p_\tau)\nu_\tau(p_{\nu_1}) \tag{34a}$$

$$\hookrightarrow V^+(Q_{2,3})\overline{\nu_\tau}(p_{\nu_2}) \tag{34b}$$

$$\hookrightarrow \pi^+(p_1)\pi^0(p_2) \tag{34c}$$

$$\pi^-(p_1)\pi^+(p_2)\pi^+(p_3). \tag{34d}$$

$$\pi^+(p_1)\pi^0(p_2)\pi^0(p_3). \tag{34e}$$

In this paper, $B \to \bar{D}$ denotes $B^0 \to D^-$ or $B^+ \to \bar{D}^0$ transitions. The differential decay rate for these processes are written as

$$d\bar{\Gamma}_n = \sum_{\lambda\lambda'} d\bar{\Gamma}_V^{\lambda\lambda'}|F_n(Q_n^2)|^2\frac{dQ_n^2}{2\pi}d\Gamma_n^{\lambda\lambda'}, \tag{35}$$

where $d\bar{\Gamma}_V^{\lambda\lambda'}$ are given as

$$d\bar{\Gamma}_V^{\lambda\lambda'} = \frac{1}{2m_B}d\Phi_4(B \to \bar{D}V\bar{\nu}\nu)\bar{\mathcal{M}}_V^\lambda\bar{\mathcal{M}}_V^{\lambda'*}, \tag{36}$$

$$\bar{\mathcal{M}}_V^\lambda = (\sqrt{2}G_F)^2 V_{cb}^* \cos\theta_C \bar{u}(p_{\nu_1})P_+\bar{\Gamma}_{\rm NP} \times \frac{-\not{p}_\tau + m_\tau}{p_\tau^2 - m_\tau^2 + im_\tau\Gamma_\tau}\gamma^\alpha P_- v(p_{\nu_2})\epsilon_\alpha^*(Q_n,\lambda), \tag{37}$$

$$\bar{\Gamma}_{\rm NP} = C_V^* H_V^\mu \gamma_\mu - C_S^* H_S - C_T^* H_T^{\mu\nu}\sigma_{\mu\nu} \quad (38)$$

$$= e^{-i\arg(C_V)}(|C_V^*| H_V^\mu \gamma_\mu - \tilde{C}_S^* H_S - \tilde{C}_T^* H_T^{\mu\nu}\sigma_{\mu\nu}). \quad (39)$$

From these equations, we obtain the following basic formula:

$$d\Gamma_n = (d\bar{\Gamma}_n^{\rm P} \text{ with } (C_V^*, C_S^*, C_T^*) \to (C_V, C_S, C_T)), \quad (40)$$

where $d\bar{\Gamma}_n^P$ denote $d\bar{\Gamma}_n$ with the parity transformation, that is, by reversing the directions of all three-momenta. In short, the distributions are CP invariant if all the Wilson coefficients are real.

Let us formally write the total amplitude, $\mathcal{M} = \sum_\lambda \mathcal{M}_V^\lambda \mathcal{M}_n^\lambda$, the product of the production (15), and decay amplitudes (24) and (25) as

$$\mathcal{M} = \mathcal{M}_{\rm SM} + C_{\rm NP}\mathcal{M}_{\rm NP}. \quad (41)$$

Here $\mathcal{M}_{\rm SM}$ is the amplitude from the SM and $C_{\rm NP}\mathcal{M}_{\rm NP}$ is the amplitude from the new physics, where $C_{\rm NP}$ denotes the Wilson coefficients of the new physics, C_V, C_S and C_T. From Eq. (40), we find

$$d\Gamma_n - d\bar{\Gamma}_n^P \propto {\rm Im}(C_{\rm NP}){\rm Im}(\mathcal{M}_{\rm SM}^* \mathcal{M}_{\rm NP}). \quad (42)$$

Therefore, we can measure the imaginary parts of the Wilson coefficients (which are the source of the CP violation) by using this asymmetry.

C. *CP*-violating observable in two-pion decay

We parametrize the momenta p_B, p_D, and Q_2 in the q rest frame ($\vec{p}_B - \vec{p}_D = \vec{0}$) as

$$p_B = \frac{\sqrt{q^2}}{2}\left(\frac{m_B^2 - m_D^2}{q^2} + 1, 0, 0, \beta\right), \quad (43)$$

$$p_D = \frac{\sqrt{q^2}}{2}\left(\frac{m_B^2 - m_D^2}{q^2} - 1, 0, 0, \beta\right), \quad (44)$$

$$Q_2 = (E_V, |\vec{p}_V|\sin\theta_V, 0, |\vec{p}_V|\cos\theta_V), \quad (45)$$

where $q = p_B - p_D$, $Q_2 = p_1 + p_2$, E_V is the sum of two pion energies, and $\beta = \bar{\beta}\left(\frac{m_B^2}{q^2}, \frac{m_D^2}{q^2}\right)$. In this frame, we define the z axis along the direction of $\vec{p}_D$ and the y axis along the direction of $\vec{p}_D \times \vec{Q}_2$. The opening angle between $\vec{p}_D$ and $\vec{Q}_2$ is denoted by θ_V. The two pion momenta p_1 and p_2 in the Q_2 rest frame ($\vec{p}_1 + \vec{p}_2 = \vec{0}$) can then be parametrized as

$$p_1 = \frac{\sqrt{Q_2^2}}{2}(1, +\beta_1 \sin\hat{\theta}_1\cos\hat{\phi}_1, +\beta_1\sin\hat{\theta}_1\sin\hat{\phi}_1, + \beta_1\cos\hat{\theta}_1), \quad (46)$$

$$p_2 = \frac{\sqrt{Q_2^2}}{2}(1, -\beta_1 \sin\hat{\theta}_1\cos\hat{\phi}_1, - \beta_1\sin\hat{\theta}_1\sin\hat{\phi}_1, -\beta_1\cos\hat{\theta}_1), \quad (47)$$

where $\beta_1 = \sqrt{1 - \frac{4m_\pi^2}{Q_2^2}}$, the z' axis is chosen along the direction of $\vec{Q}_2$ in the q rest frame, and the y' axis is the same as the y axis. The polar and azimuthal angle of $\vec{p}_1, \hat{\theta}_1$, and $\hat{\phi}_1$, are parametrized as shown in Fig. 1. We define the polarization vectors of the vector resonance in this Q_2 rest frame as

$$\epsilon(\pm) = \frac{1}{\sqrt{2}}(0, \mp 1, -i, 0), \quad (48)$$

$$\epsilon(0) = (0, 0, 0, 1), \quad (49)$$

and the density-matrix distribution of the vector resonance decay in the case of $V \to 2\pi$ is

$$\frac{d\Gamma_2^{\lambda\lambda'}}{d\cos\hat{\theta}_1 d\hat{\phi}_1} = G_2(Q_2^2)\mathcal{D}^{\lambda\lambda'}(\cos\hat{\theta}_1, \hat{\phi}_1), \quad (50)$$

$$G_2(Q_2^2) = \frac{Q_2^2}{16\pi^2}\sqrt{1 - \frac{4m_\pi^2}{Q_2^2}}, \quad (51)$$

with

$$\mathcal{D}^{\lambda\lambda'}(\cos\theta, \phi) = \begin{pmatrix} \frac{\sin^2\theta}{2} & \frac{-\sin^2\theta e^{2i\phi}}{2} & \frac{-\sin 2\theta e^{i\phi}}{2\sqrt{2}} \\ \frac{-\sin^2\theta e^{-2i\phi}}{2} & \frac{\sin^2\theta}{2} & \frac{\sin 2\theta e^{-i\phi}}{2\sqrt{2}} \\ \frac{-\sin 2\theta e^{-i\phi}}{2\sqrt{2}} & \frac{\sin 2\theta e^{i\phi}}{2\sqrt{2}} & \cos^2\theta \end{pmatrix}. \quad (52)$$

Here $\lambda(\lambda') = +1, -1, 0$ from the top rows (left columns), and the diagonal elements are simply the square of the d functions, $d^{J=1}_{\lambda,0}(\theta)$.

Let us define the density matrix of the vector resonance production after integrating out the momenta of the two unmeasurable neutrinos as

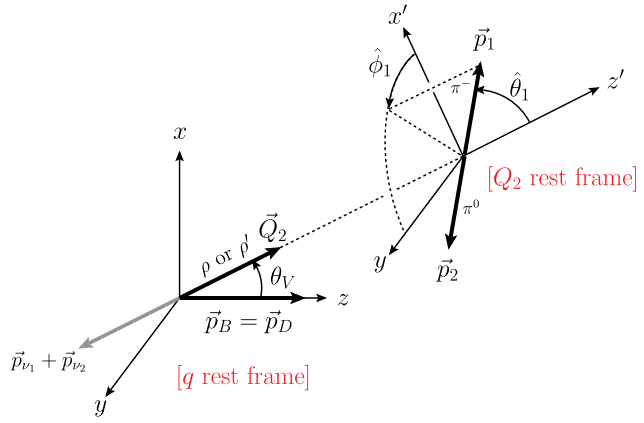

FIG. 1 (color online). The kinematics in the case of $V \to 2\pi$.

$$\mathcal{P}^{\lambda\lambda'}(q^2, E_V, \cos\theta_V, Q_n^2) = \left.\frac{d\Gamma_V^{\lambda\lambda'}}{dq^2 dE_V d\cos\theta_V}\right|_{m_V^2 = Q_n^2}. \tag{53}$$

We can now write the differential decay rate for all measurable momenta as

$$\frac{d\Gamma_2}{dq^2 dE_V d\cos\theta_V dQ_2^2 d\cos\hat{\theta}_1 d\hat{\phi}_1} = \sum_{\lambda,\lambda'} \mathcal{P}_2^{\lambda\lambda}(q^2, E_V, \cos\theta_V, Q_2^2)\mathcal{D}^{\lambda\lambda}(\cos\hat{\theta}_1, \hat{\phi}_1), \tag{54}$$

where

$$\mathcal{P}_2^{\lambda\lambda} = \mathcal{P}^{\lambda\lambda}(q^2, E_V, \cos\theta_V, Q_2^2)\frac{1}{2\pi}|F_2(Q_2^2)|^2 G_2(Q_2^2). \tag{55}$$

From Eq. (52), we obtain the following equation:

$$\begin{aligned}\frac{d\Gamma_2}{dq^2 dE_V d\cos\theta_V dQ_2^2 d\cos\hat{\theta}_1 d\hat{\phi}_1} &= (\mathcal{P}_2^{++} + \mathcal{P}_2^{--})\frac{\sin^2\hat{\theta}_1}{2} + \mathcal{P}_2^{00}\cos^2\hat{\theta}_1 - \mathrm{Re}(\mathcal{P}_2^{+-})\sin^2\hat{\theta}_1\cos 2\hat{\phi}_1 - \mathrm{Re}(\mathcal{P}_2^{+0} + \mathcal{P}_2^{-0}) \\ &\times \frac{\sin 2\hat{\theta}_1\cos\hat{\phi}_1}{\sqrt{2}.} + \mathrm{Im}(\mathcal{P}_2^{+-})\sin^2\hat{\theta}_1\sin 2\hat{\phi}_1 + \mathrm{Im}(\mathcal{P}_2^{+0} + \mathcal{P}_2^{-0})\frac{\sin 2\hat{\theta}_1\sin\hat{\phi}_1}{\sqrt{2}}.\end{aligned} \tag{56}$$

The differential decay rate of the *CP*-conjugate process $B \to \bar{D}\pi^+\pi^0\nu_\tau\bar{\nu}_\tau$—where all the three-momenta are reversed—differs from Eq. (56) by only the last two terms,

$$\begin{aligned}&\frac{d\Gamma_2 - d\bar{\Gamma}_2^{\mathrm{P}}}{dq^2 dE_V d\cos\theta_V dQ_2^2 d\cos\hat{\theta}_1 d\hat{\phi}_1} \\ &= 2\mathrm{Im}(\mathcal{P}_2^{+-})\sin^2\hat{\theta}_1\sin 2\hat{\phi}_1 \\ &\quad + 2\mathrm{Im}(\mathcal{P}_2^{+0} + \mathcal{P}_2^{-0})\frac{\sin 2\hat{\theta}_1\sin\hat{\phi}_1}{\sqrt{2}}.\end{aligned} \tag{57}$$

Here $\hat{\theta}_1$ and $\hat{\phi}_1$ for π^+ are defined exactly the same as for π^- in Eq. (46). It should be noted here that the last two terms in Eq. (56) change sign under parity transformation. The *CP*-violating term hence appears as a *P*-odd distribution in the process $\bar{B} \to D\pi^-\pi^0\nu_\tau\bar{\nu}_\tau$, and it reverses the sign for the *CP*-conjugate process $B \to \bar{D}\pi^+\pi^0\nu_\tau\bar{\nu}_\tau$.

Actually, the sensitivity of $\mathrm{Im}(\mathcal{P}_2^{+-})$ to the imaginary parts of the Wilson coefficients [$C_{V,S,T}$ of Eq. (16), or, more precisely speaking, the phase of $\tilde{C}_{T,S}$ in Eq. (18), since the phase of C_V is unobservable in our approximation] turns out to be very small compared with that of $\mathrm{Im}(\mathcal{P}_2^{+0} + \mathcal{P}_2^{-0})$. Therefore, we discuss only the asymmetry due to the last term of Eq. (57). We define the q^2- and E_V-dependent asymmetry distribution after integrating over all the other kinematical variables as follows:

$$A_2(q^2, E_V) \equiv \frac{1}{\Gamma_2 + \bar{\Gamma}_2}\int d\cos\theta_V dQ_2^2\left(\int_0^1 - \int_{-1}^0\right)d\cos\hat{\theta}_1\left(\int_0^\pi - \int_\pi^{2\pi}\right)d\hat{\phi}_1\frac{d\Gamma_2 - d\bar{\Gamma}_2^{\mathrm{P}}}{dq^2 dE_V d\cos\theta_V dQ_2^2 d\cos\hat{\theta}_1 d\hat{\phi}_1} \tag{58}$$

$$= \frac{32}{3\sqrt{2}(\Gamma_2 + \bar{\Gamma}_2)}\int d\cos\theta_V dQ_2^2 \mathrm{Im}(\mathcal{P}_2^{+0} + \mathcal{P}_2^{-0}), \tag{59}$$

where Γ_2 and $\bar{\Gamma}_2$ are the total decay rate of the processes $\bar{B} \to D\pi^-\pi^0\nu_\tau\bar{\nu}_\tau$ and $B \to \bar{D}\pi^+\pi^-\nu_\tau\bar{\nu}_\tau$, respectively.

D. *CP*-violating observable in three-pion decay

The amplitude of $a_1 \to 3\pi$ is

$$\begin{aligned}\mathcal{M}_3^\lambda &= \frac{4}{3f_\pi}\epsilon^\alpha(Q_3, \lambda)[F_2(P_{12}^2)(p_1 - p_2)_\alpha \\ &\quad + F_2(P_{13}^2)(p_1 - p_3)_\alpha].\end{aligned} \tag{60}$$

The contribution of this amplitude becomes large when P_{12}^2 or P_{13}^2 are near the pole of the ρ meson. When both P_{12} and P_{13} are near the pole, the amplitude is enhanced. Roughly half of the distribution falls in the region. On the double ρ-meson pole, the $a_1 \to 3\pi$ decay amplitude is written as

$$\begin{aligned}\mathcal{M}_3^\lambda|_{P_{12}^2 = P_{13}^2 = m_\rho^2} &= \frac{4}{3f_\pi}\epsilon^\alpha(Q_3, \lambda)[F_2(m_\rho^2)(p_1 - p_2)_\alpha \\ &\quad + F_2(m_\rho^2)(p_1 - p_3)_\alpha]\end{aligned} \tag{61}$$

$$\sim \frac{4}{3f_\pi}\epsilon^\alpha(Q_3,\lambda)\left[\frac{im_\rho}{\Gamma_\rho}(p_1-p_2)_\alpha+\frac{im_\rho}{\Gamma_\rho}(p_1-p_3)_\alpha\right] \quad (62)$$

$$=\frac{4}{3f_\pi}\frac{2im_\rho}{\Gamma_\rho}\epsilon^\alpha(Q_3,\lambda)\left(p_1-\frac{p_2+p_3}{2}\right)_\alpha. \quad (63)$$

This has the same momentum structure as that of $V\to 2\pi$. Furthermore, under the CP transformation, both $\vec{p}_1$ and $(\vec{p}_2+\vec{p}_3)/2$ change sign, because we assign p_2 and p_3 for two identical π's consistently for all 3π decay modes; see Eqs. (12d) and (12e) for a_1^- and Eqs. (34d) and (34e) for a_1^+. Therefore we can define the CP asymmetry in exactly the same way as in the $V\to 2\pi$ case by retaining only the sum of the two identical π's momenta in the three-body phase space. This definition is applicable even when only one of either P_{12}^2 or P_{13}^2 is near the pole of the ρ meson, as shown in the Appendix.

We parametrize the momenta Q_3 in the q rest frame as

$$Q_3=(E_V,|\vec{p}_V|\sin\theta_V,0,|\vec{p}_V|\cos\theta_V), \quad (64)$$

where E_V is the sum of three pion energies. The parametrization of p_B and p_D and the definition of the axis directions are the same as those of $V\to 2\pi$; see Eqs. (43)–(45). The opening angle made by $\vec{p}_D$ and $\vec{Q}_3$ is denoted by θ_V. Then, we parametrize the momenta p_1 and P_{23} in the Q_3 rest frame ($\vec{p}_1+\vec{p}_2+\vec{p}_3=\vec{0}$) as

$$p_1=\frac{\sqrt{Q_3^2}}{2}\left(1+\frac{m_\pi^2}{Q_3^2}-\frac{P_{23}^2}{Q_3^2},+\beta_1'\sin\hat{\theta}_1\cos\hat{\phi}_1 +\beta_1'\sin\hat{\theta}_1\sin\hat{\phi}_1,+\beta_1'\cos\hat{\theta}_1\right), \quad (65)$$

$$P_{23}=\frac{\sqrt{Q_3^2}}{2}\left(1+\frac{P_{23}^2}{Q_3^2}-\frac{m_\pi^2}{Q_3^2},-\beta_1'\sin\hat{\theta}_1\cos\hat{\phi}_1 -\beta_1'\sin\hat{\theta}_1\sin\hat{\phi}_1,-\beta_1'\cos\hat{\theta}_1\right), \quad (66)$$

where $\beta_1'=\bar{\beta}\left(\frac{m_\pi^2}{Q_3^2},\frac{P_{23}^2}{Q_3^2}\right)$ and $P_{23}=p_2+p_3$. In this frame, we define the z' axis as the direction of $\vec{Q}_3$ in the q rest frame, and the y' axis as the direction of the y axis. The polar and azimuthal angle of $\vec{p}_1$, $\hat{\theta}_1$, and $\hat{\phi}_1$ are parametrized as shown in Fig. 2. With this approximation, the decay density matrix has the same form as in Eq. (52) for a given P_{23}^2 after integrating over the internal phase space that keeps P_{23}. We therefore arrive at the CP asymmetry for the 3π process, which has the same form as in Eq. (57),

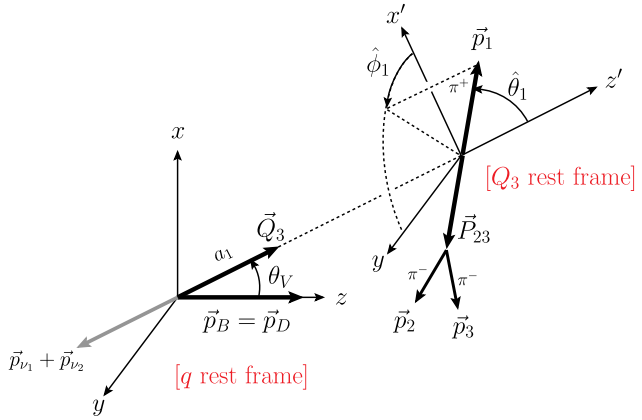

FIG. 2 (color online). The kinematics in the case of $V\to 3\pi$.

$$A_3(q^2,E_V)\equiv\frac{1}{\Gamma_3+\bar{\Gamma}_3}\int d\cos\theta_V dQ_3^2 \times\left(\int_0^1-\int_{-1}^0\right)d\cos\hat{\theta}_1\left(\int_0^\pi-\int_\pi^{2\pi}\right)d\hat{\phi}_1 \times\frac{d\Gamma_3-d\bar{\Gamma}_3^{\mathrm{P}}}{dq^2dE_V d\cos\theta_V dQ_3^2 d\cos\hat{\theta}_1 d\hat{\phi}_1}, \quad (67)$$

where Γ_3 and $\bar{\Gamma}_3$ denote the total decay width of $\bar{B}\to D(3\pi)\nu_\tau\bar{\nu}_\tau$ and $B\to\bar{D}(3\pi)\nu_\tau\bar{\nu}_\tau$, respectively. In the above equation, the integration over the invariant mass P_{23}^2 and the internal two-body (p_2+p_3) phase space has been suppressed for brevity. Although we can define a more sophisticated CP asymmetry for the 3π mode by making full use of the three-body decay kinematics (see, e.g., Ref. [39]), we find that the above simple asymmetry has a sufficiently strong sensitivity to CP violation, as shown in the next section.

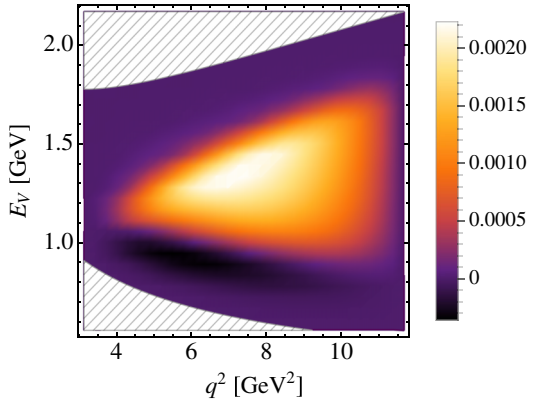

FIG. 3 (color online). Density plot of the CP-asymmetry function $A_2(q^2,E_V)$ in $C_S=i$ and $C_V=C_T=0$. The shaded areas are prohibited kinematically.

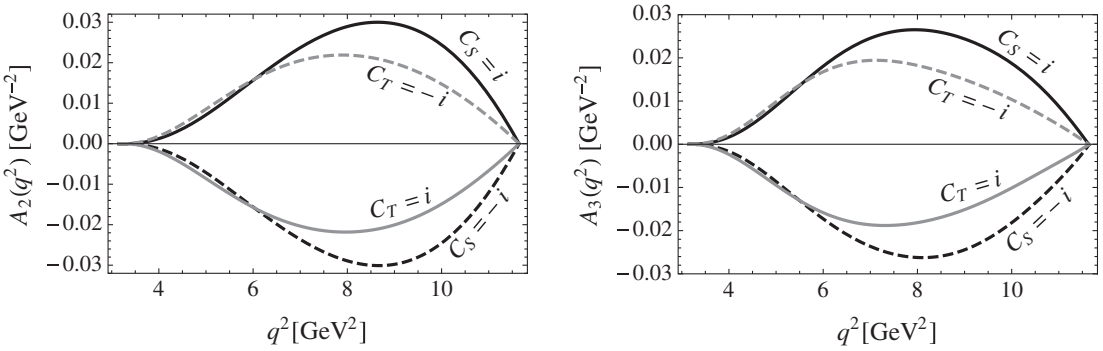

FIG. 4. The CP-asymmetry distributions $A_n(q^2) = \int dE_V A_n(q^2, E_V)$ for the $2\pi(n = 2)$ mode (left) and the $3\pi(n = 3)$ mode (right). The black solid curves show results for $(C_V, C_S, C_T) = (0, i, 0)$, the black dashed curves are for $(0, -i, 0)$, the gray solid curves are for $(0, 0, i)$, and the gray dashed curves are for $(0, 0, -i)$.

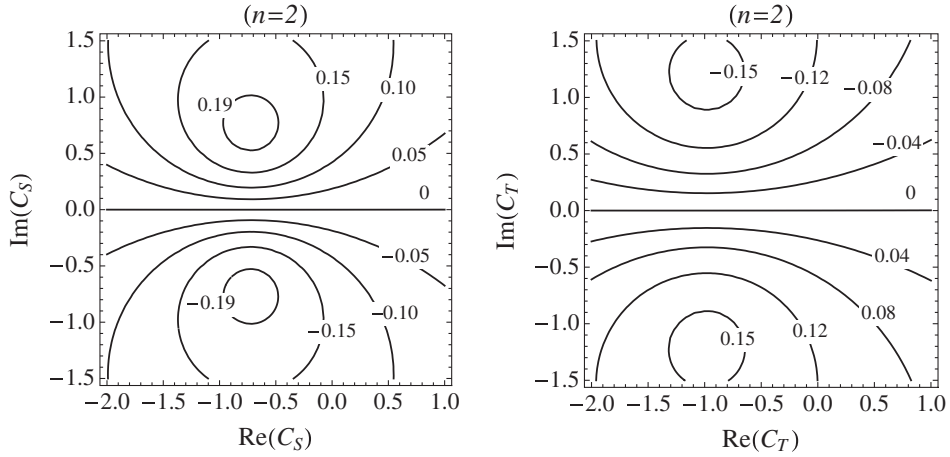

FIG. 5. Contour plots of the integrated CP asymmetry, $A_2 = \int dq^2 dE_V A_2(q^2, E_V)$, on the plane of complex coefficients C_S (left) and C_T (right), when all the other Wilson coefficients are set to zero.

III. NUMERICAL RESULTS

A. Model-independent analysis

We estimate the sensitivity of the distributions A_2 and A_3 to the imaginary parts of the new physics Wilson coefficients.

In Fig. 3, we show the density plot of the CP-asymmetry function $A_2(q^2, E_V)$ in $C_S = i$ and $C_V = C_T = 0$. The shaded areas are prohibited kinematically. The shape of the density distributions are same for other values of C_S. In the tensor case, the distribution slightly differs from that of C_S. In the case of $\mathrm{Im}(C_{S,T}) = 0$, the distribution is zero over all of the phase space.

In Fig. 4, we show the distributions $A_n(q^2) = \int dE_V A_n(q^2, E_V)$ for the $2\pi(n = 2)$ mode (left) and for the $3\pi(n = 3)$ mode (right). The black solid curves show results for $(C_V, C_S, C_T) = (0, i, 0)$, the black dashed curves are for $(0, -i, 0)$, the gray solid curves are for $(0, 0, i)$, and the gray dashed curves are for $(0, 0, -i)$. The shapes of the distributions for the scalar effect are different from those for the tensor effect. Therefore, we can discriminate the type of the new physics interaction that induces the CP violation by using these q^2 distributions. When the sign of the imaginary part changes, the signs of the distributions also change. Note that the signs of the distributions for the 2π and 3π modes are the same for each of the models. So, an unwanted cancellation does not happen even if the $2\pi^0$'s in the $a_1 \to \pi^\pm\pi^0\pi^0$ decay are not resolved; then, it should contribute to the $\rho \to \pi^\pm\pi^0$-mode analysis.

In Figs. 5 and 6, we show contour plots of the integrated CP asymmetry, $A_n = \int dq^2 dE_V A_n(q^2, E_V)$, on the plane of the complex coefficients C_S (left) and C_T (right), when all the other Wilson coefficients are set to zero. The typical values are about 0.1 on $\mathrm{Im}(C_{S,T}) \simeq 0.5$ for both A_2 and A_3.[4] There are other integrated observables, for example, τ and D^* polarizations [3,8,11] and forward-backward asymmetries [5,9]. The behavior of the A_n for the Wilson coefficients are different from such observables.

[4]In this paper, we do not discuss uncertainties in A_2 and A_3 arising from nonresonant contributions and the pion rescattering.

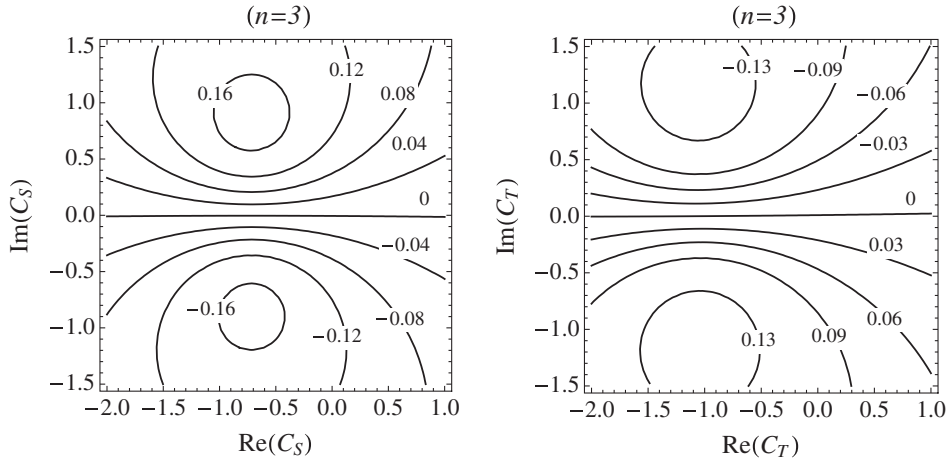

FIG. 6. Contour plots of the integrated CP asymmetry, $A_3 = \int dq^2 dE_V A_3(q^2, E_V)$, on the plane of complex coefficients C_S (left) and C_T (right), when all the other Wilson coefficients are set to zero.

Therefore, the A_n are useful to make the constraints on the Wilson coefficients tight. It is notable that the A_n decide the sign of the imaginary part of the Wilson coefficients.

B. Model analysis

It has been shown that the leptoquark models and the type-III 2HDM could potentially explain the present experimental data. So, we examine predictions for the size of the CP violation for these models.

1. Leptoquark models

Some leptoquark models have a parameter space that explain the experimental data [9]. In this paper, we consider three leptoquark models as follows:

$$\mathcal{L}_{R_2} = (h^{ij}_{2L}\bar{u}_{iR}L_{jL} + h^{ij}_{2R}\bar{Q}_{iL}i\sigma_2 l_{jR})R_2, \tag{68}$$

$$\mathcal{L}_{S_1} = (g^{ij}_{1L}\bar{Q}^c_{iL}i\sigma_2 L_{jL} + g^{ij}_{1R}\bar{u}^c_{iR}l_{jR})S_1, \tag{69}$$

$$\mathcal{L}_{V_2} = (g^{ij}_{2L}\bar{d}^c_{iR}\gamma^\mu L_{jL} + g^{ij}_{2R}\bar{Q}^c_{iL}\gamma^\mu l_{jR})V_2. \tag{70}$$

The quantum numbers of the leptoquarks are summarized in Table I. Then, the Wilson coefficients of these leptoquarks are given as

$$C_{V_1} = \frac{1}{2\sqrt{2}G_F V_{cb}}\sum_{k=1}^{3} V_{k3}\frac{g^{k3}_{1L}g^{23*}_{1L}}{2M^2_{S_1^{1/3}}}, \tag{71}$$

$$C_{S_1} = \frac{-1}{2\sqrt{2}G_F V_{cb}}\sum_{k=1}^{3} V_{k3}\frac{2g^{k3}_{2L}g^{23*}_{2R}}{M^2_{V_2^{1/3}}}, \tag{72}$$

$$C_{S_2} = \frac{-1}{2\sqrt{2}G_F V_{cb}}\sum_{k=1}^{3} V_{k3}\left(\frac{h^{23}_{2L}h^{k3*}_{2R}}{2M^2_{R_2^{2/3}}} + \frac{g^{k3}_{1L}g^{23*}_{1R}}{2M^2_{S_1^{1/3}}}\right), \tag{73}$$

$$C_T = \frac{-1}{2\sqrt{2}G_F V_{cb}}\sum_{k=1}^{3} V_{k3}\left(\frac{h^{23}_{2L}h^{k3*}_{2R}}{8M^2_{R_2^{2/3}}} - \frac{g^{k3}_{1L}g^{23*}_{1R}}{8M^2_{S_1^{1/3}}}\right). \tag{74}$$

It is interesting that the R_2 and S_1 leptoquark models produce the combinations of the scalar and tensor interactions. The favored imaginary parts of the product of couplings for these leptoquark models with a leptoquark mass of 1 TeV have been estimated in Ref. [9] as

$$1.92 < |\mathrm{Im}(h^{23}_{2L}h^{33*}_{2R})| < 2.42 \quad (R_2 \text{ leptoquark}), \tag{75}$$

$$1.92 < |\mathrm{Im}(g^{33}_{1L}g^{23*}_{1R})| < 2.42 \quad (S_1 \text{ leptoquark}), \tag{76}$$

$$0.34 < |\mathrm{Im}(g^{33}_{2L}g^{23*}_{2R})| < 0.68 \quad (V_2 \text{ leptoquark}). \tag{77}$$

In Fig. 7, we show the CP-asymmetry distributions $A_n(q^2) = \int dE_V A_n(q^2, E_V)$ for these couplings in Eqs. (75)–(77). The black (dark gray) [light gray] curve shows the distribution in the R_2 (S_1) [V_2] leptoquark model. We set the sign of the imaginary part of the coupling product for the R_2 (S_1) [V_2] leptoquark to $-$ ($-$) [$+$]. Central values of the integrated CP asymmetry, $A_n = \int dq^2 dE_V A_n(q^2, E_V)$, for these couplings are shown in Table II. The signs of the A_n are opposite those of the imaginary part of the coupling products for each case.

TABLE I. Quantum numbers of the R_2, S_1, and V_2 leptoquarks with $\mathrm{SU}(3)_c \times \mathrm{SU}(2)_L \times U(1)_Y$-invariant couplings.

	R_2	S_1	V_2
spin	0	0	1
$F = 3B + L$	0	-2	-2
$\mathrm{SU}(3)_c$	3	3^*	3^*
$\mathrm{SU}(2)_L$	2	1	2
$U(1)_{Y=Q-T_3}$	7/6	1/3	5/6

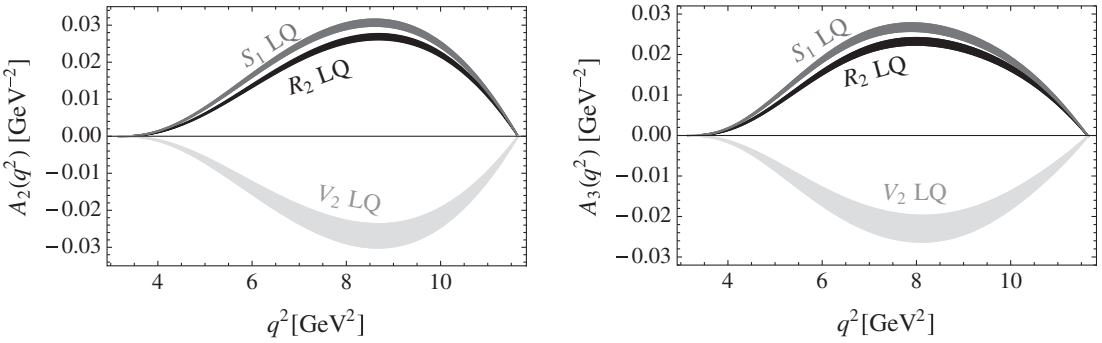

FIG. 7. The *CP*-asymmetry distributions $A_n(q^2) = \int dE_V A_n(q^2, E_V)$ for the product of couplings in the range given in Eqs. (75)–(77). The black (dark gray) [light gray] curve shows the distribution in the R_2 (S_1) [V_2] leptoquark model. We set the sign of the imaginary part of the coupling product for the R_2 (S_1) [V_2] leptoquark to $-$ ($-$) [$+$].

In fact, the allowed regions for the present experimental data in the R_2 leptoquark model exist only around the region in Eq. (75). So, if *CP* violation is not observed, the R_2 leptoquark model would be completely excluded.

2. Type III 2HDM

The 2HDMs predict charged Higgs bosons $H^\pm$ which affect the decay $B \to D\tau\nu$ at tree level. The Lagrangian including the charged Higgs boson in the type-III 2HDM is written as

$$\mathcal{L}_{H^\pm} = \frac{1}{v}\left[\bar{u}_{iR}\left(\cot\beta m_{u_i}\delta_{ij} - \frac{v}{\sin\beta}\epsilon^{U*}_{ji}\right)V^{\rm CKM}_{jk} d_{kL}\right. \quad (78)$$

$$+\bar{u}_{iL}V^{\rm CKM}_{ij}\left(\tan\beta m_{d_j}\delta_{jk} - \frac{v}{\cos\beta}\epsilon^{D}_{jk}\right)d_{kR} \quad (79)$$

$$\left.+\bar{\nu}_{iL}\left(\tan\beta m_{l_i}\delta_{ij} - \frac{v}{\cos\beta}\epsilon^{E}_{ij}\right)l_{jR}\right]H^+ + \text{H.c.}, \quad (80)$$

where $v = 174$ GeV and $V^{\rm CKM}$ denotes the Cabibbo-Kobayashi-Maskawa matrix. Then, the Wilson coefficients of this model are

$$C_{S_1} = -\left(\tan\beta m_b - \frac{v}{V_{cb}\cos\beta}\epsilon^{D}_{23}\right) \times \left(\tan\beta m_\tau - \frac{v}{\cos\beta}\epsilon^{E*}_{23}\right)\frac{1}{m^2_{H^\pm}}, \quad (81)$$

TABLE II. Central values of the integrated *CP* asymmetry, $A_n = \int dq^2 dE_V A_n(q^2, E_V)$, for the couplings in Eq. (75)–(77). The signs of the A_n are opposite that of the imaginary part of the coupling products for each case.

	R_2	S_1	V_2
A_2	∓ 0.13	∓ 0.15	∓ 0.13
A_3	∓ 0.11	∓ 0.13	∓ 0.11

$$C_{S_2} = -\left(\cot\beta m_c - \frac{v}{V_{cb}\sin\beta}\epsilon^{U*}_{32}\right) \times \left(\tan\beta m_\tau - \frac{v}{\cos\beta}\epsilon^{E*}_{23}\right)\frac{1}{m^2_{H^\pm}}, \quad (82)$$

where $V_{cb} \equiv V^{\rm CKM}_{j3}$, and we use the approximation $V^{\rm CKM}_{j3} \simeq \delta_{j3}$. The off-diagonal elements of the matrices ϵ^U, ϵ^D, and ϵ^E induce the flavor-changing neutral current, so the constraints on these parameters are tight. Actually, the constraint on the parameters ϵ^D_{23} and ϵ^E_{23} are tight, so we neglect these parameters. However, the constraint on the ϵ^U_{32} is not so tight, and there is an allowed region for this parameter, which has been shown in Ref. [24].

In this paper, we set $\tan\beta = 50$ and $m_{H^\pm} = 500$ GeV. In Fig. 8, the black region shows the allowed region for the experimental data of $R(D)$ and $R(D^*)$ on the parameter ϵ^U_{32} at 2σ level. The gray region shows the allowed region at the 2σ level for the normalized q^2 distribution in $\bar{B} \to D\tau(\to \ell\nu\bar{\nu})\bar{\nu}$ with the kinematic cut $m^2_{\rm miss} > 1.5$ GeV^2,

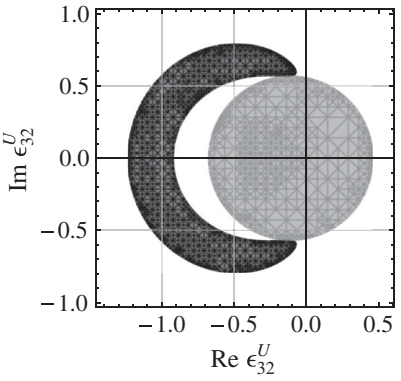

FIG. 8. The black region shows the allowed region for the experimental data of $R(D)$ and $R(D^*)$ on the parameter ϵ^U_{32} at the 2σ level. The gray region shows the allowed region for the normalized q^2 distribution in $\bar{B} \to D\tau(\to \ell\nu\bar{\nu})\bar{\nu}$ with the kinematic cut $m^2_{\rm miss} > 1.5$ GeV^2 at the 2σ level. We set $\tan\beta = 50$ and $m_{H^\pm} = 500$ GeV.

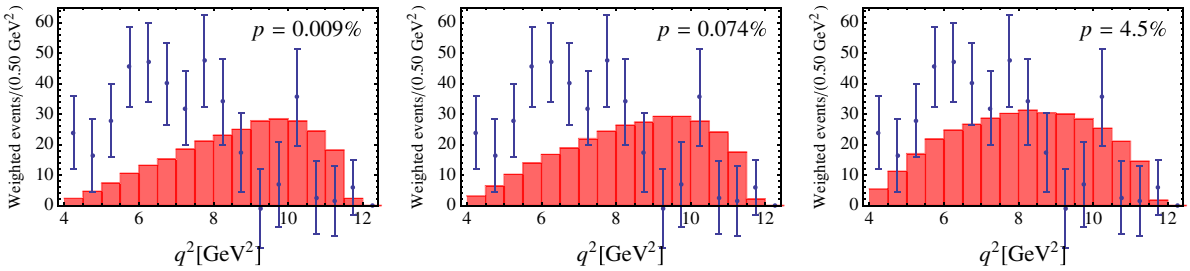

FIG. 9 (color online). The left (center) [right] histogram shows the theoretical prediction of the normalized q^2 distribution with the cut for the parameter $\epsilon_{32}^U = -1$ ($\epsilon_{32}^U = -0.7 \pm 0.6i$) [$\epsilon_{32}^U = -0.13 \pm 0.57i$] and the experimental data. The uncertainty on the data points includes the statistical uncertainties of data and simulation. The p-value for each parameter is shown.

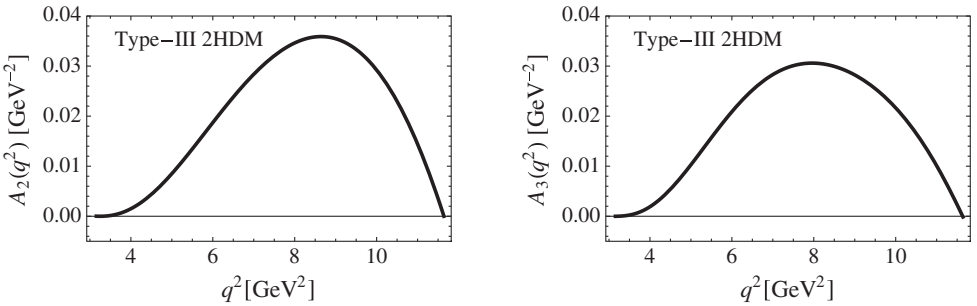

FIG. 10. The left (right) panel shows the CP-asymmetry distributions $A_2(q^2)$ ($A_3(q^2)$) on $\epsilon_{32}^U = -0.13 - 0.57i$.

which was measured by the *BABAR* Collaboration [13]. This kinematic cut is the same as that of *BABAR*. In Fig. 9, the left (center) [right] histogram shows the theoretical prediction of the normalized q^2 distribution with the cut for the parameter $\epsilon_{32}^U = -1$ ($\epsilon_{32}^U = -0.7 \pm 0.6i$) [$\epsilon_{32}^U = -0.13 \pm 0.57i$] and the experimental data. The uncertainty on the data points includes the statistical uncertainties of data and simulation. The p-value for each parameter is also shown. Please see Ref. [40] for more details about the q^2 distribution analysis.

It does not seem that the type-III 2HDM is consistent with the experimental results. However, the p-values for the normalized q^2 distribution on $\epsilon_{32}^U = -0.13 \pm 0.57i$ (which are the boundaries of the black and gray regions) are larger than those in the allowed region for $R(D^{(*)})$. So, we assume these parameters as benchmark points in the type-III 2HDM.

In Fig. 10, the left (right) figure shows the CP-asymmetry distributions $A_2(q^2)$ ($A_3(q^2)$) on $\epsilon_{32}^U = -0.13 - 0.57i$, and the integrated CP asymmetry A_n on $\epsilon_{32}^U = -0.13 \pm 0.57i$ are shown in Table III. The signs of the A_n are opposite that of the imaginary part of the parameter ϵ_{32}^U.

TABLE III. The integrated CP asymmetry A_n on $\epsilon_{32}^U = -0.13 \pm 0.57i$. The signs of the A_n are opposite that of the imaginary part of the parameter ϵ_{32}^U.

	type-III 2HDM
A_2	∓ 0.17
A_3	∓ 0.15

IV. CONCLUSION

In this paper, we have constructed the CP-asymmetry distribution $A_2(q^2, E_V)$ for the decay processes $B \to D\tau(\to 2\pi)\nu_\tau$ and $A_3(q^2, E_V)$ for $B \to D\tau(\to 3\pi)\nu_\tau$ by using the polarization of the vector resonances produced by the tau lepton. Assuming that the tau neutrinos are left-handed, we have introduced the general effective Hamiltonian that contains all possible four-fermion operators of the lowest dimension for $b \to c\tau\nu_\tau$. The two independent imaginary parts of the parameters $\tilde{C}_S$ and $\tilde{C}_T$ given by the Wilson coefficients of these operators induce the CP violation and nonzero distributions of $A_n(q^2, E_V)$. These two parameters are related with the non-standard-model scalar and tensor interactions.

We have examined the sensitivities of the $A_n(q^2, E_V)$ to the scalar and tensor interactions. The shapes of the CP-aymmetric q^2 distribution, $A_n(q^2) = \int A_n(q^2, E_V)$, for the scalar interaction are different from those of the tensor interaction. Therefore, we can discriminate the type of the new physics interaction that induces the CP violation using the distributions. The integrated CP asymmetries, $A_n = \int dq^2 dE_V A_n(q^2, E_V)$, are also sensitive to $\mathrm{Im}(\tilde{C}_{S,T})$, and are typically about 0.1 on $\mathrm{Im}(C_{S,T}) \simeq 0.5$ for both 2π and 3π decays.

Some new physics models have been considered to explain the discrepancy between the present experimental

data and the SM predictions, and these would induce CP violation. We have examined the expected CP violation for three leptoquark models. The favored imaginary parts of the coupling products in the leptoquark models are known, and we have estimated the $A_n(q^2)$ and A_n for these couplings. The allowed regions for the present experimental data in the R_2 leptoquark model only exist on the nonzero imaginary part. So, if CP violation in $B \to D\tau\nu$ is not observed, the R_2 leptoquark model would be completely excluded.

We have also discussed the type-III 2HDM, and indicated the inconsistency of this model by using the experimental data for the ratios of the measured branching fractions $R(D^{(*)})$ and the normalized q^2 distribution in $\bar{B} \to D\tau\bar{\nu}$. Assuming the parameters $\epsilon_{32}^U = -0.13 \pm 0.57i$ as benchmark points in this model, we have estimated the $A_n(q^2)$ and A_n in the type-III 2HDM.

In conclusion, the past measurements for $B \to D\tau\nu$ by the *BABAR* and Belle Collaborations used only the leptonic tau decay modes, $\tau \to \ell\nu\bar{\nu}$. An analysis using the hadronic tau decay modes in semitauonic B decays would be difficult; however, they would offer a great amount of information about the tau lepton polarization. We hope for successful measurements of the hadronic channels at Belle-II and LHCb.

ACKNOWLEDGMENTS

We thank Ryoutaro Watanabe for very helpful discussions, and also Toru Goto, Junya Nakamura, and Minoru Tanaka for useful comments. This work is supported by the Grant-in-Aid for Scientific Research from the Ministry of Education, Science, Sports, and Culture (MEXT), Japan (25400287 and 23104006).

APPENDIX: SINGLE ρ-MESON-POLE APPROXIMATION

In Sec. II D, we explained that the decay density matrix for $V \to 3\pi$ has the same form as for $V \to 2\pi$ in Eq. (52) when P_{12}^2 and P_{13}^2 are both near the pole of the ρ meson. In this appendix, we show that the correspondence between $V \to 3\pi$ and $V \to 2\pi$ is also approximately applicable even when only one of either P_{12}^2 or P_{13}^2 is near the invariant mass squared of the ρ meson. The magnitude of the distribution in this phase space is comparable with that on the double ρ-meson pole, which is discussed in Sec. II D.

The first (second) term in the square bracket in Eq. (25) is dominant when P_{12}^2 (P_{13}^2) is near the pole and P_{13}^2 (P_{12}^2) is far away from the pole. The decay density matrix distribution for $V \to 3\pi$ in these phase space regions is written approximately as

$$\begin{aligned} d\Gamma_3^{\lambda\lambda'} \simeq \int \frac{16\pi m_\rho}{9 f_\pi^2 \Gamma_\rho} [& d\Phi_3 \delta(P_{12}^2 - m_\rho^2) \\ & \times \epsilon_\alpha(Q_3, \lambda)(p_1 - p_2)^\alpha \epsilon_{\alpha'}^*(Q_3, \lambda') \\ & \times (p_1 - p_2)^{\alpha'} + (2 \to 3)]. \end{aligned} \tag{A1}$$

We assume that the momentum squared P_{13}^2 (P_{12}^2) in the first (second) term that is not near the pole is significantly smaller than m_ρ^2. After integrating over the momentum squared P_{23}^2 and the two-body $(p_2 + p_3)$ phase space for massless pions, we obtain the following equation:

$$\frac{d\Gamma_3^{\lambda\lambda'}}{d\cos\hat{\theta}_1 d\hat{\phi}_1} \simeq G_3(Q_3^2) \tilde{\mathcal{D}}^{\lambda\lambda'}(\cos\hat{\theta}_1, \hat{\phi}_1), \tag{A2}$$

$$G_3(Q_3^2) = \frac{(1+r)m_\rho^3}{576\pi^3 f_\pi^2 \Gamma_\rho}, \tag{A3}$$

with

$$\tilde{\mathcal{D}}^{\lambda\lambda'}(\cos\theta, \phi) = \frac{1}{3\delta} \begin{pmatrix} \frac{\sin^2\theta}{2} + \delta & \frac{-\sin^2\theta e^{2i\phi}}{2} & \frac{-\sin 2\theta e^{i\phi}}{2\sqrt{2}} \\ \frac{-\sin^2\theta e^{-2i\phi}}{2} & \frac{\sin^2\theta}{2} + \delta & \frac{\sin 2\theta e^{-i\phi}}{2\sqrt{2}} \\ \frac{-\sin 2\theta e^{-i\phi}}{2\sqrt{2}} & \frac{\sin 2\theta e^{i\phi}}{2\sqrt{2}} & \cos^2\theta + \delta \end{pmatrix}, \tag{A4}$$

where $\delta = (1+r)/7r^2$ and $r = m_\rho^2/Q_3^2$. The off-diagonal elements of the decay density matrix $\tilde{\mathcal{D}}^{\lambda\lambda'}$ are proportional to those for $V \to 2\pi$ in Eq. (52). The differential decay rate $d\Gamma_3$ has a similar form as $d\Gamma_2$ in Eq. (56) due to the above equations. Therefore, using the CP asymmetry defined in Eq. (67), we can measure the coefficient function $\mathrm{Im}(\mathcal{P}^{+0} + \mathcal{P}^{-0})$ that measures CP violation.

[1] U. Nierste, S. Trine, and S. Westhoff, Phys. Rev. D **78**, 015006 (2008).
[2] J. F. Kamenik and F. Mescia, Phys. Rev. D **78**, 014003 (2008).
[3] M. Tanaka and R. Watanabe, Phys. Rev. D **82**, 034027 (2010).
[4] S. Fajfer, J. F. Kamenik and I. Nisandzic, Phys. Rev. D **85**, 094025 (2012).
[5] Y. Sakaki and H. Tanaka, Phys. Rev. D **87**, 054002 (2013).
[6] J. A. Bailey *et al.*, Phys. Rev. Lett. **109**, 071802 (2012).
[7] D. Becirevic, N. Kosnik, and A. Tayduganov, Phys. Lett. B **716**, 208 (2012).
[8] M. Tanaka and R. Watanabe, Phys. Rev. D **87**, 034028 (2013).
[9] Y. Sakaki, M. Tanaka, A. Tayduganov, and R. Watanabe, Phys. Rev. D **88**, 094012 (2013).
[10] W.-S. Hou, Phys. Rev. D **48**, 2342 (1993).

[11] M. Tanaka, Z. Phys. C **67**, 321 (1995).
[12] J. P. Lees *et al.* (BABAR Collaboration), Phys. Rev. Lett. **109**, 101802 (2012).
[13] J. P. Lees *et al.* (BABAR Collaboration), Phys. Rev. D **88**, 072012 (2013).
[14] A. Matyja *et al.* (Belle Collaboration), Phys. Rev. Lett. **99**, 191807 (2007).
[15] I. Adachi *et al.* (Belle Collaboration), arXiv:0910.4301.
[16] A. Bozek *et al.* (Belle Collaboration), Phys. Rev. D **82**, 072005 (2010).
[17] A. Datta, M. Duraisamy, and D. Ghosh, Phys. Rev. D **86**, 034027 (2012).
[18] S. Fajfer, J. F. Kamenik, I. Nisandzic, and J. Zupan, Phys. Rev. Lett. **109**, 161801 (2012).
[19] A. Celis, M. Jung, X.-Q. Li, and A. Pich, J. High Energy Phys. 01 (2013) 054.
[20] P. Ko, Y. Omura and C. Yu, J. High Energy Phys. 03 (2013) 151.
[21] P. Biancofiore, P. Colangelo, and F. De Fazio, Phys. Rev. D **87**, 074010 (2013).
[22] A. Celis, M. Jung, X.-Q. Li, and A. Pich, J. Phys. Conf. Ser. **447**, 012058 (2013).
[23] I. Dorsner, S. Fajfer, N. Kosnik, and I. Nisandzic, J. High Energy Phys. 11 (2013) 084.
[24] A. Crivellin, C. Greub, and A. Kokulu, Phys. Rev. D **86**, 054014 (2012).
[25] M. Duraisamy and A. Datta, J. High Energy Phys. 09 (2013) 059.
[26] B. Aubert *et al.* (BABAR Collaboration), Phys. Rev. D **77**, 032002 (2008).
[27] B. Aubert *et al.* (BABAR Collaboration), Phys. Rev. D **79**, 012002 (2009).
[28] W. Dungel *et al.* (Belle Collaboration), Phys. Rev. D **82**, 112007 (2010).
[29] S. Jadach, J. H. Kuhn, and Z. Was, Comput. Phys. Commun. **64**, 275 (1991).
[30] M. Jezabek, Z. Was, S. Jadach, and J. H. Kuhn, Comput. Phys. Commun. **70**, 69 (1992).
[31] R. Barate *et al.* (ALEPH Collaboration), Eur. Phys. J. C **4**, 409 (1998).
[32] M. Fujikawa *et al.* (Belle Collaboration), Phys. Rev. D **78**, 072006 (2008).
[33] Y. Amhis *et al.* (Heavy Flavor Averaging Group), arXiv:1207.1158.
[34] A. Datta, K. Kiers, D. London, P. J. O'Donnell, and A. Szynkman, Phys. Rev. D **75**, 074007 (2007); **76**079902(E) (2007).
[35] K. Kiers, K. Little, A. Datta, D. London, M. Nagashima, and A. Szynkman, Phys. Rev. D **78**, 113008 (2008).
[36] I. Caprini, L. Lellouch, and M. Neubert, Nucl. Phys. **B530**, 153 (1998).
[37] K. Abe *et al.* (Belle Collaboration), Phys. Lett. B **526**, 258 (2002).
[38] K. Hagiwara, T. Li, K. Mawatari, and J. Nakamura, Eur. Phys. J. C **73**, 2489 (2013).
[39] S. Y. Choi, K. Hagiwara, and M. Tanabashi, Phys. Rev. D **52**, 1614 (1995).
[40] Y. Sakaki, M. Tanaka, A. Tayduganov, and R. Watanabe (to be published).